IRIS SENSOR TESTS: an Interim Report

– by –

Robert A. Uhrhammer
and
T. V. McEvilly

Berkeley Seismological Laboratory

Email: bob@seismo.berkeley.edu

Poster Presentation
2001 IRIS Workshop
(revised 20 June 2001)

Introduction

The Berkeley Seismological Laboratory (BSL) has set up an instrumentation test facility in the Byerly Seismographic Vault (BKS) in order to systematically determine and to compare the characteristics of up to eight sensors at a time. The test instrumentation consists of an eight channel Quanterra Q4128 data logger and a custom interconnect panel that provides isolated power and preamplification when required in order to facilitate the interconnection and routing of the signals from the sensors to the data logger with shielded signal lines. Upon acquisition of 100 sps data from the instruments under test, Power Spectral Density (PSD) analysis is used to characterize and compare the performance of each sensor. Tilt tests and seismic signals with a sufficient signal level above the background seismic noise are also used to verify the absolute calibration of the sensors. During the initial tests, we characterized the eight sensors shown in Table 1.

Table 1 – Sensors

Manufacturer	Model	Serial Number
Wilcoxon	X731B	P01
PMD	MET[1]	none
Streckeisen	STS–2[2]	20022
Endevco	86	AA01
MEMS	SF1500A	358
Kinemetrics	Episensor	812
Wilcoxon	9XL[3]	P002
RefTek	131–02	251

Note:

1 – New MET sensor but without feedback circuitry.
2 – STS–2 used as reference for comparison.
3 – aka IRIS SUMS.

Table 2 – Sensor Transduction Constants

Sensor	Sensitivity (w/ preamp)	Sensitivity (sensor) (V/g)
X731B	41.7 V/(m/s^2)	4.26
MET	1960 V/(m/s)	–
STS–2	1500 V/(m/s)	–
86	74.4[1] V/(m/s^2)	7.29
SF1500A	0.152 V/(m/s^2)	1.49
Episensor	7.59 V/(m/s^2)	74.4
9XL	24.2[1] V/(m/s^2)	2.37
131–02	97.1[2] V/(m/s^2)	2.38

Note:

1 – Includes 100x preamplification.
2 – Includes 400x preamplification.

Figure 1 – Plot of raw data sample which includes P–wave from a recent major teleseism (M 7, 2001.154.0241, Kermedec Is., depth 191 km, distance 85 degrees). Note the wide variation in the signal characteristics which is due to differences in the sensor sensitivity, transduction, and noise characteristics. In Figures 1–3, the sensor–channel mapping is:

Sensor	Channel
X731B	HH1
MET	HH2
Sensor A	HH3
STS–2	HH4
Sensor B	HH5
Sensor C	HH6
Episensor	HH7
Sensor D	HH8

Figure 1

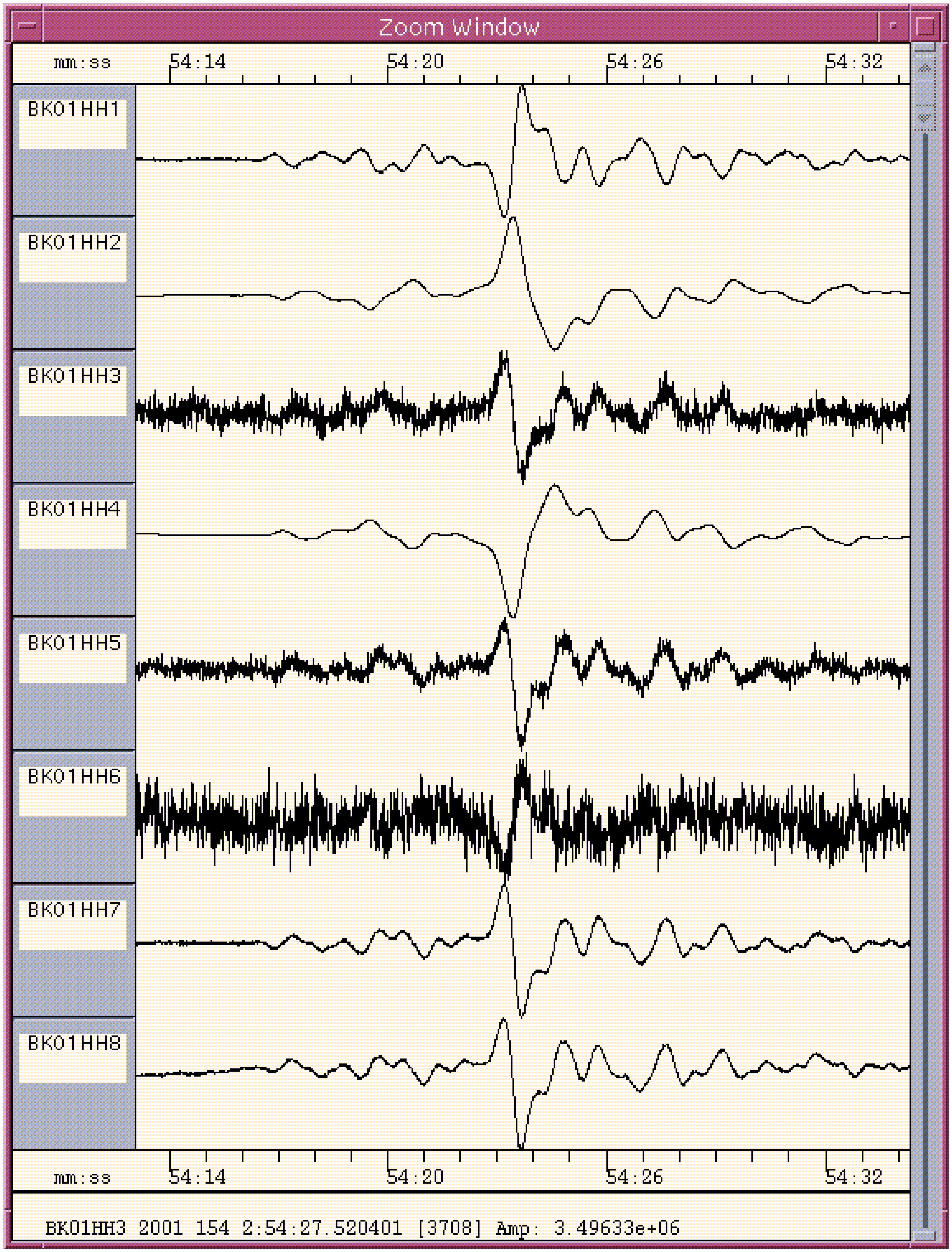
Zoom Window
mm:ss
54:14
54:20
54:26
54:32
BK01HH1
BK01HH2
BK01HH3
BK01HH4
BK01HH5
BK01HH6
BK01HH7
BK01HH8
BK01HH3 2001 154 2:54:27.520401 [3708] Amp: 3.49633e+06

Figure 2 – Comparison of absolute ground accelerations inferred from the signals recorded by each of the eight sensors. Note the variation in the signal−to−noise ratio (SNR) and frequency characteristics of each sensor. The peak signal in the middle of the plot is the P−wave from the teleseism. See Figure 1 caption for sensor−channel mapping.

Figure 2

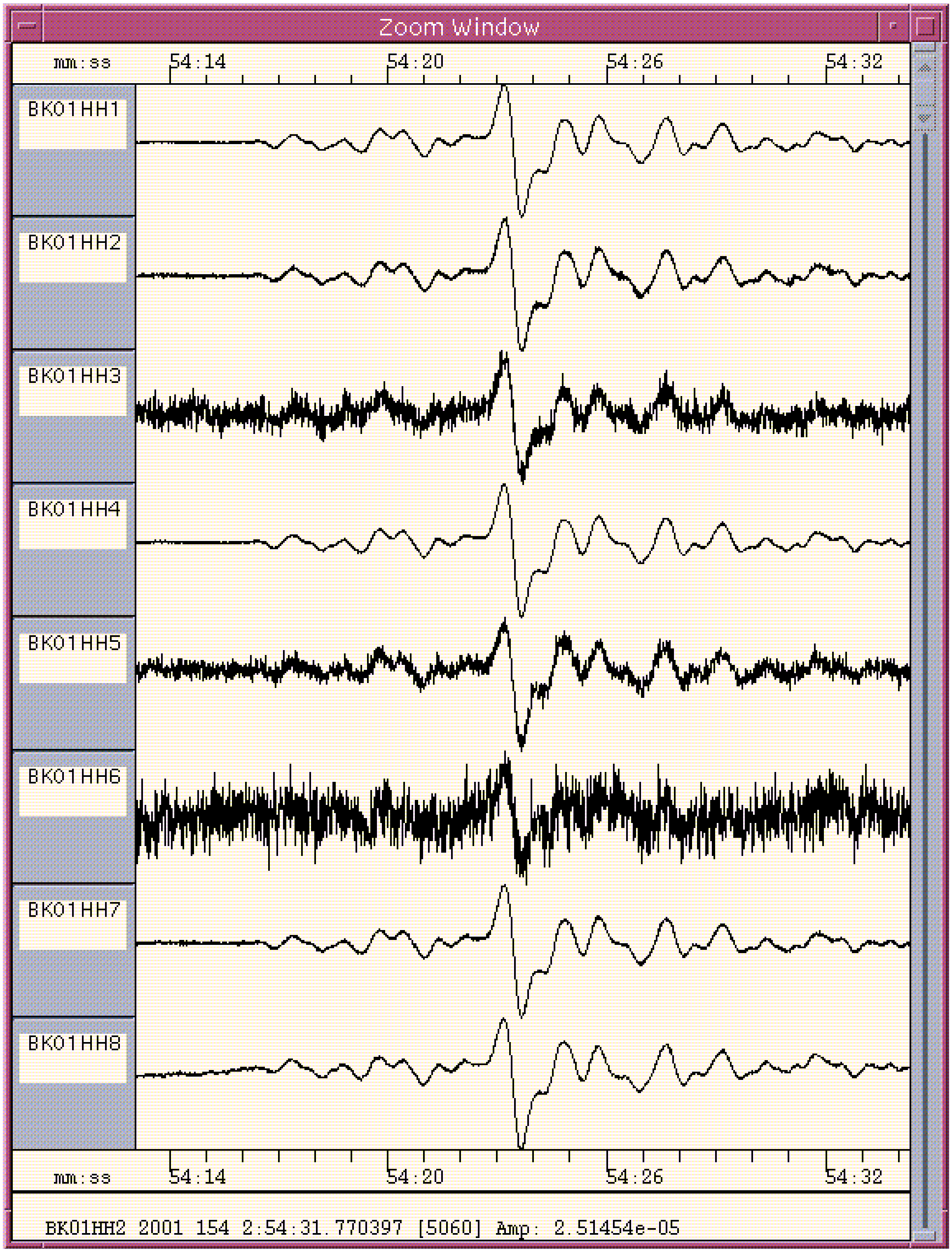
Zoom Window
mm:ss
54:14
54:20
54:26
54:32
BK01HH1
BK01HH2
BK01HH3
BK01HH4
BK01HH5
BK01HH6
BK01HH7
BK01HH8
BK01HH2 2001 154 2:54:31.770397 [5060] Amp: 2.51454e-05

Figure 3 – Data from Figure 2 which has been 0.3–2 Hz bandpass filtered to enhance the SNR of the teleseismic P–wave. The eight traces are plotted on an absolute scale and the P–P signal level is 335 u/s^2 (0.0335 gal) (–87 dB PSD in the 0.3–2 Hz band). Note that all sensors recorded the P–wave and that the sensors with the highest noise PSD levels (as shown in Figures 4a–h) exhibit a degraded SNR. The transduction constant for each of the sensors under test was empirically determined by comparing their inferred ground acceleration against the ground acceleration inferred from the STS–2 recording and the results are given in Table 2. See Figure 1 caption for sensor–channel mapping.

Figure 3

Zoom Window
mm:ss
54:14
54:20
54:26
54:32
BK01HH1
BK01HH2
BK01HH3
BK01HH4
BK01HH5
BK01HH6
BK01HH7
BK01HH8
BK01HH1 2001 154 2:54:33.980400 [6206] Amp: -1.09985e-05

Figures 4a–h – Background noise PSD plots for each of the eight sensors. Each plot shows PSD estimates from six 45–minute long time series taken hourly starting at 2001.152.0500. The scales are all identical. For reference, the background noise PSD plot (except in Figure 4d) for each sensor includes the STS–2 noise PSD estimates shown as dashed lines. Since this is a interim report and the manufacturers have not yet seen the results, the sensors on loan to BSL for testing are identified only as sensors A, B, C, and D. The PSD algorithm used in this study is the one that has been developed for IRIS by Uhrhammer.

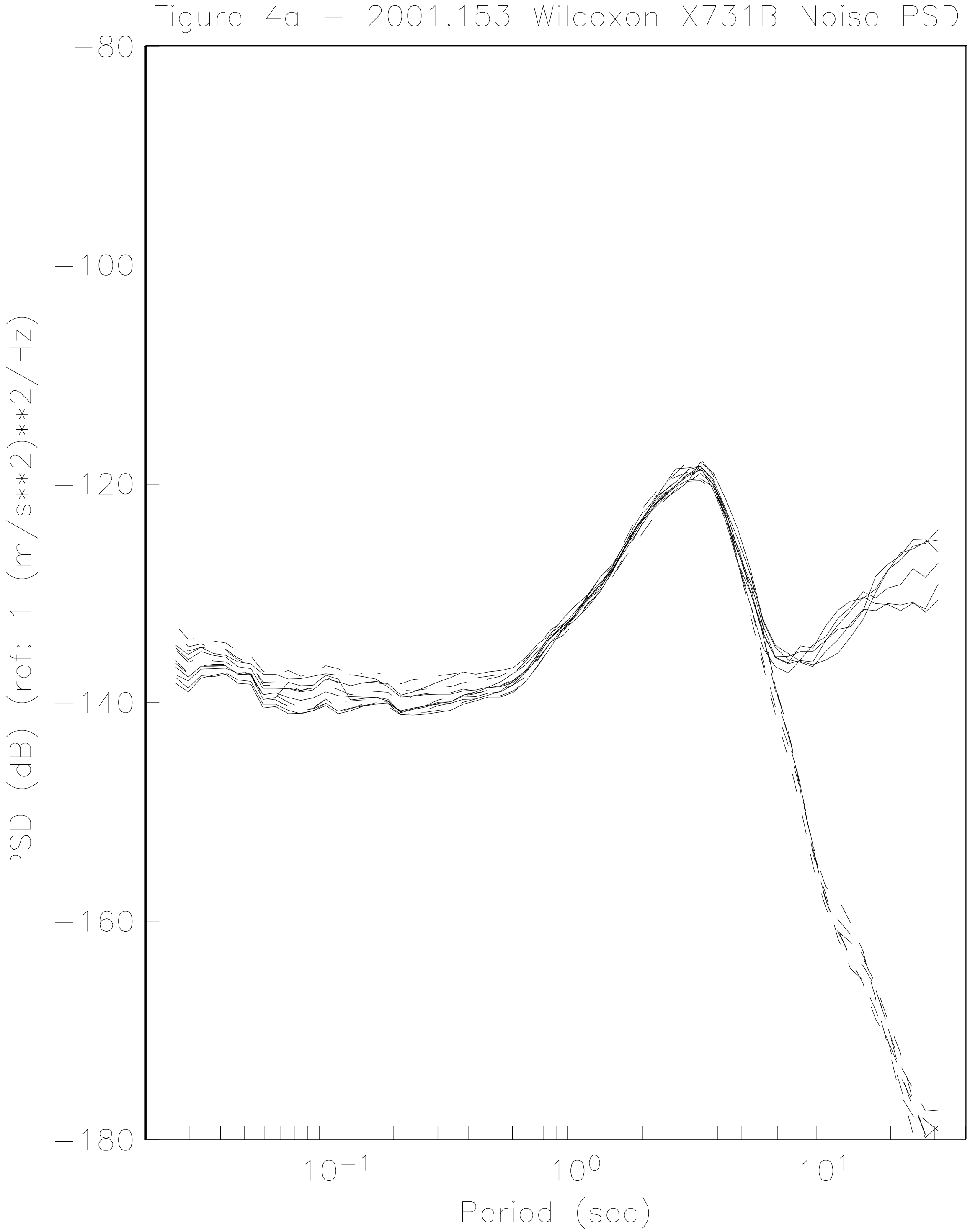
Figure 4a – 2001.153 Wilcoxon X731B Noise PSD
−80
−100
−120
−140
−160
−180
PSD (dB) (ref: 1 (m/s**2)**2/Hz)
10^{-1}
10^{0}
10^{1}
Period (sec)

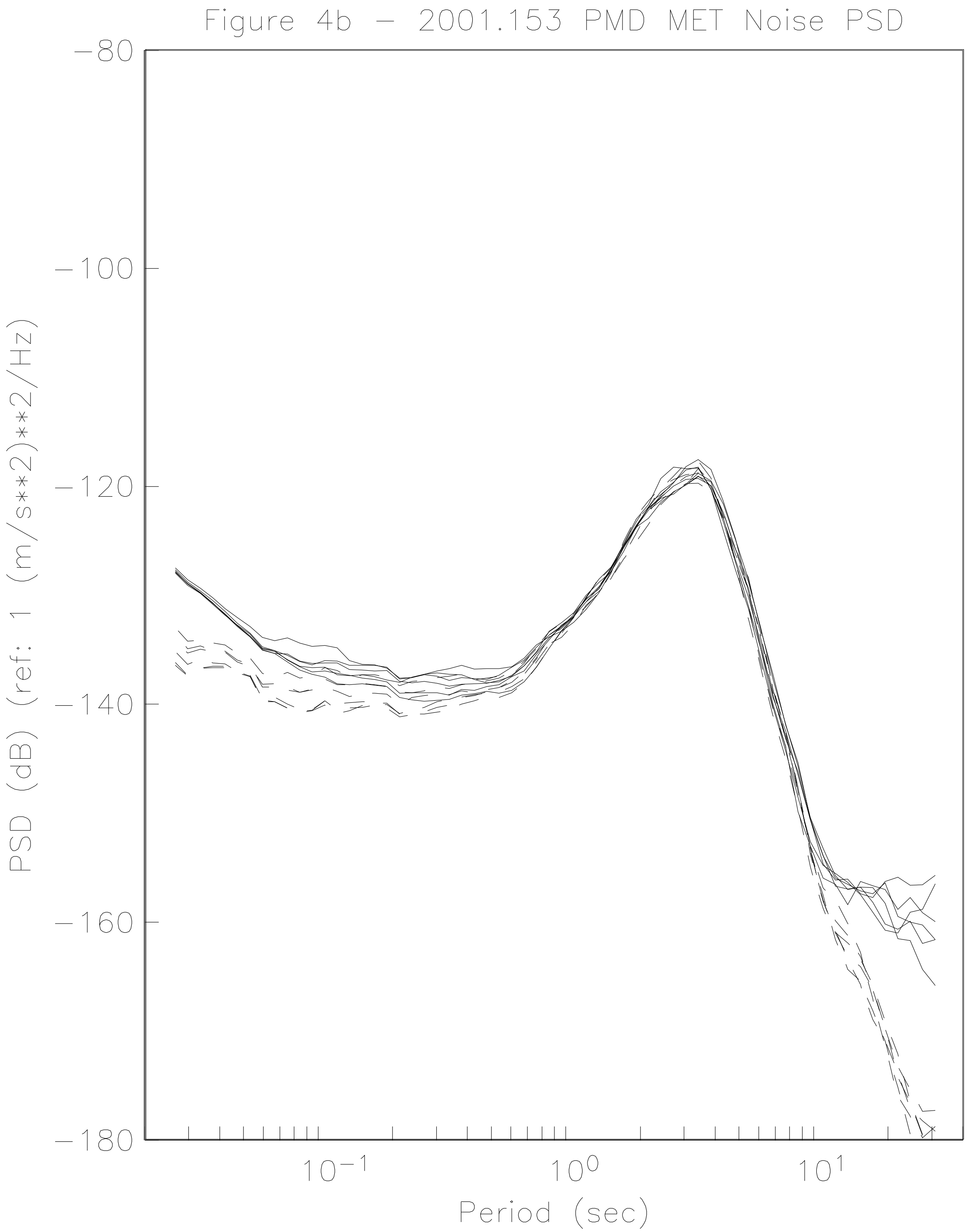
Figure 4b – 2001.153 PMD MET Noise PSD
-80
-100
-120
-140
-160
-180
PSD (dB) (ref: 1 (m/s**2)**2/Hz)
10^{-1}
10^{0}
10^{1}
Period (sec)

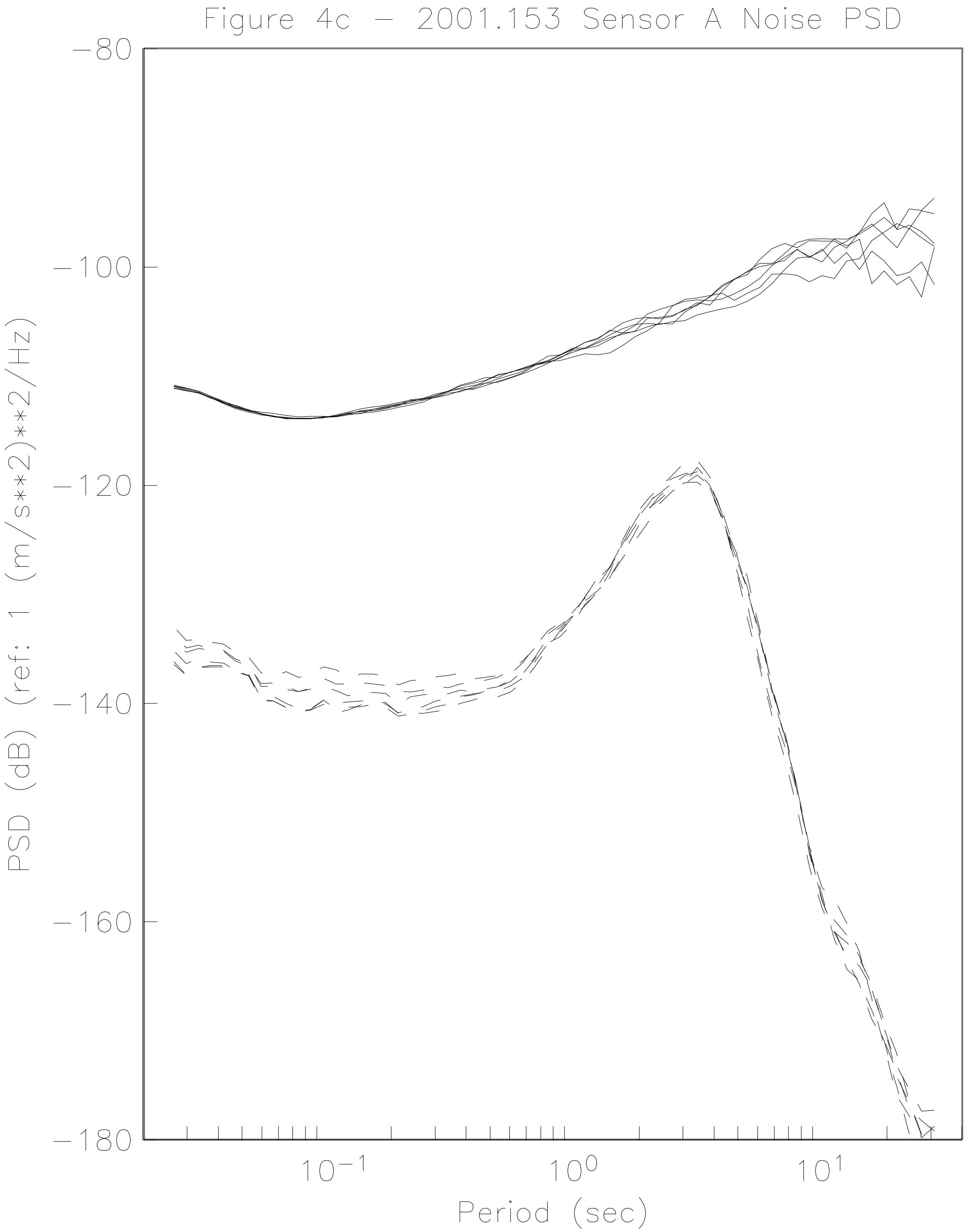
Figure 4c – 2001.153 Sensor A Noise PSD
PSD (dB) (ref: 1 (m/s**2)**2/Hz)
−80
−100
−120
−140
−160
−180
10^{-1}
10^{0}
10^{1}
Period (sec)

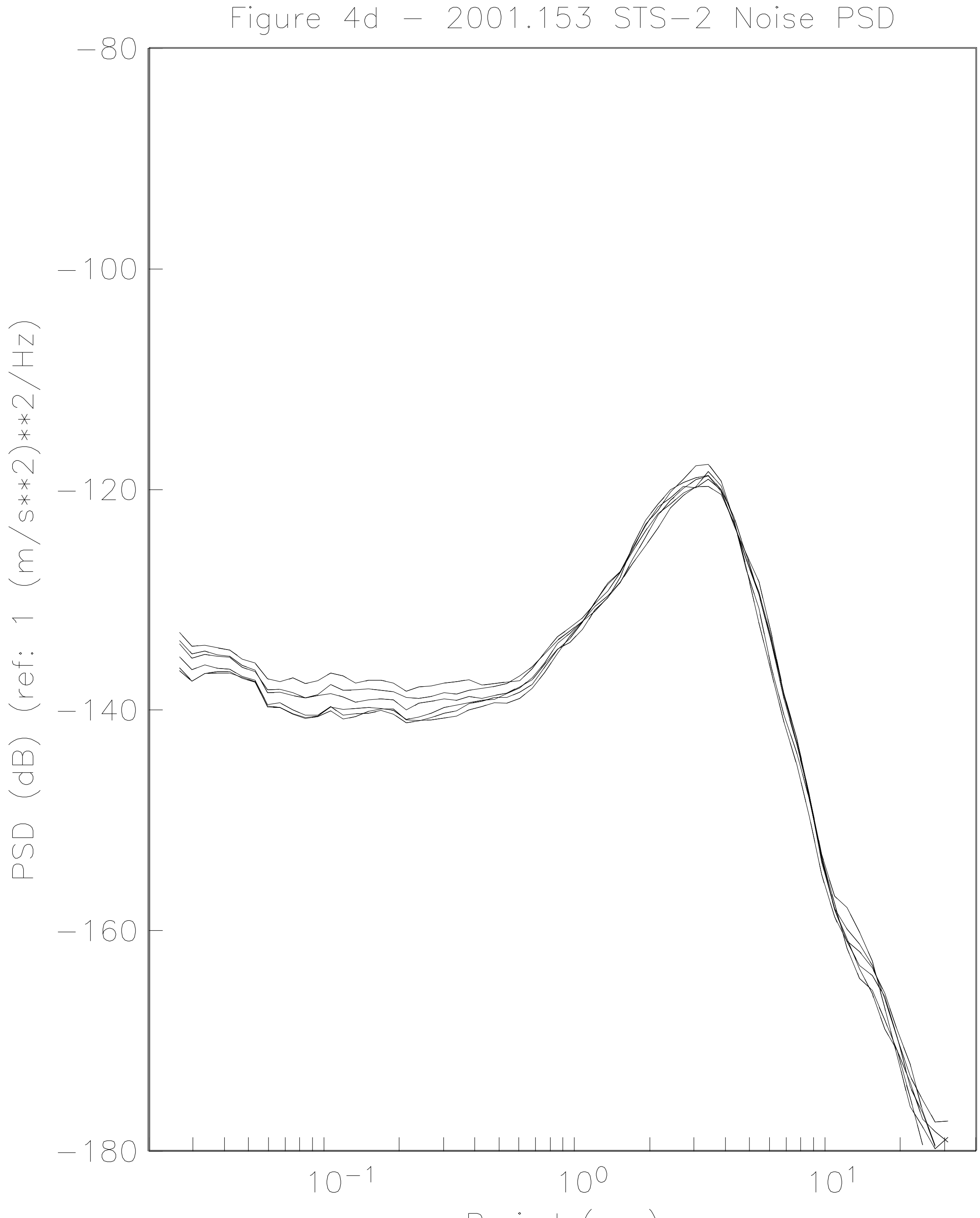
Figure 4d – 2001.153 STS-2 Noise PSD
PSD (dB) (ref: 1 (m/s**2)**2/Hz)
−80
−100
−120
−140
−160
−180
10^{-1}
10^{0}
10^{1}
Period (sec)

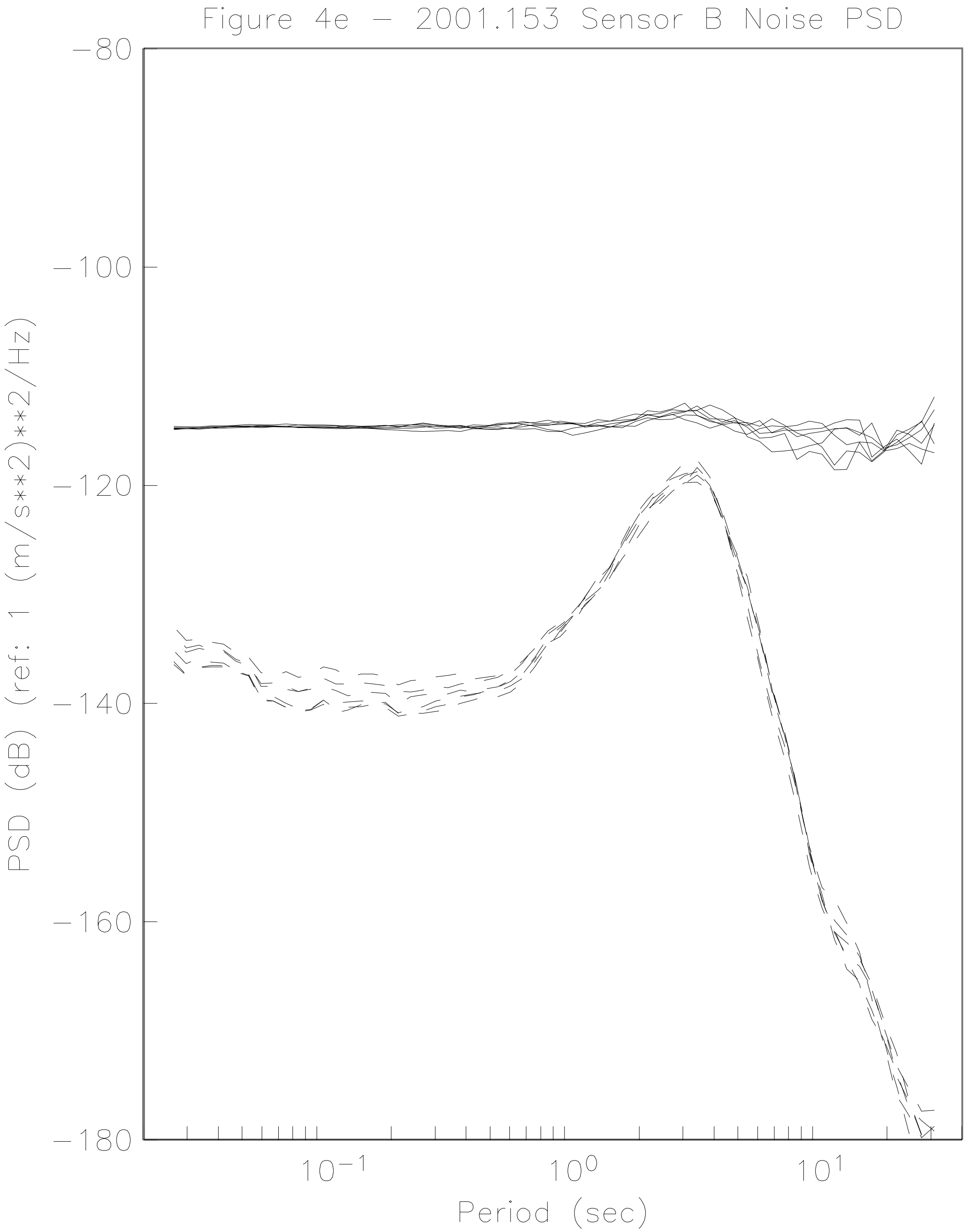
Figure 4e – 2001.153 Sensor B Noise PSD
-80
-100
-120
-140
-160
-180
PSD (dB) (ref: 1 (m/s**2)**2/Hz)
10^-1
10^0
10^1
Period (sec)

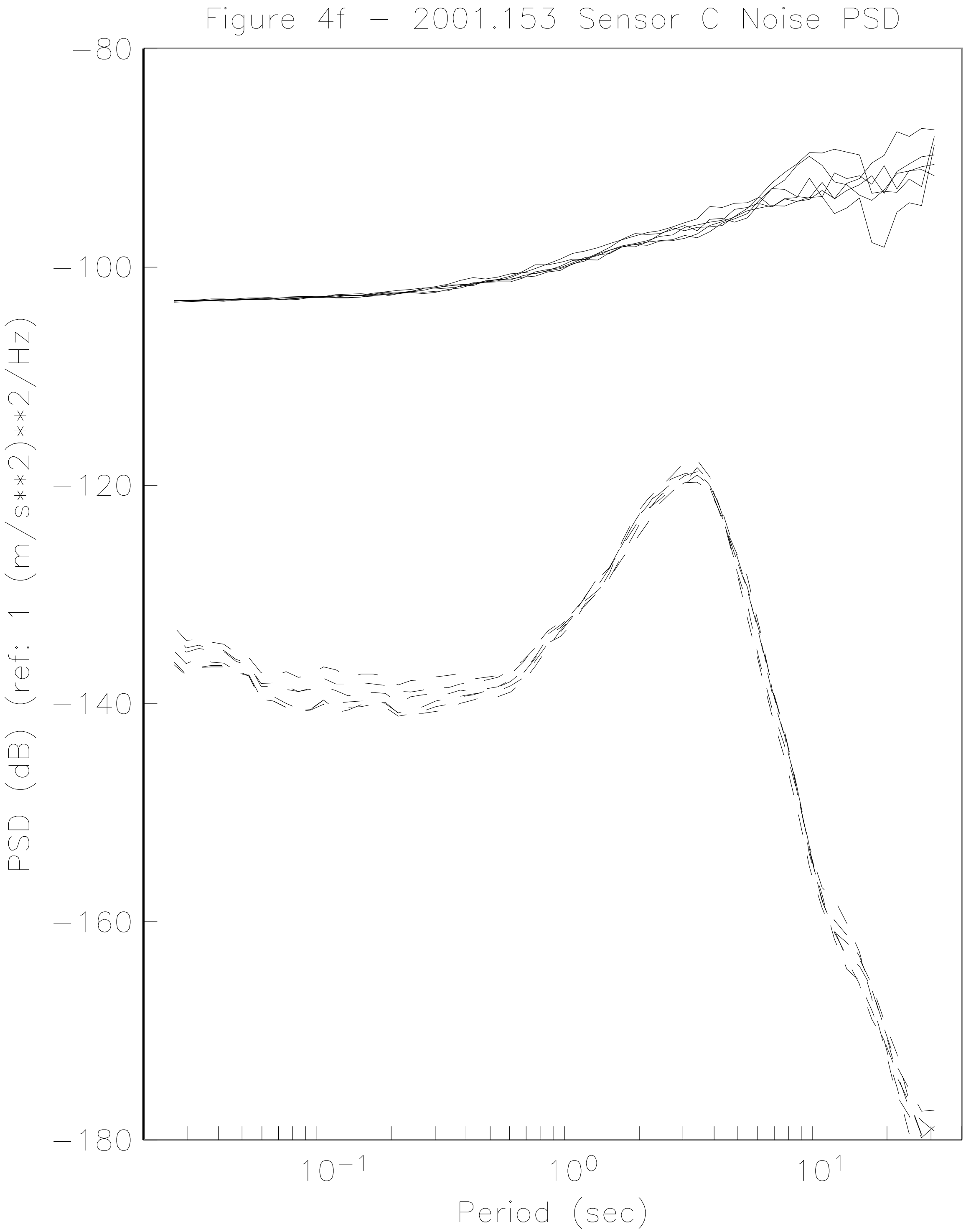
Figure 4f – 2001.153 Sensor C Noise PSD
PSD (dB) (ref: 1 (m/s**2)**2/Hz)
Period (sec)
-80
-100
-120
-140
-160
-180
10^{-1}
10^{0}
10^{1}

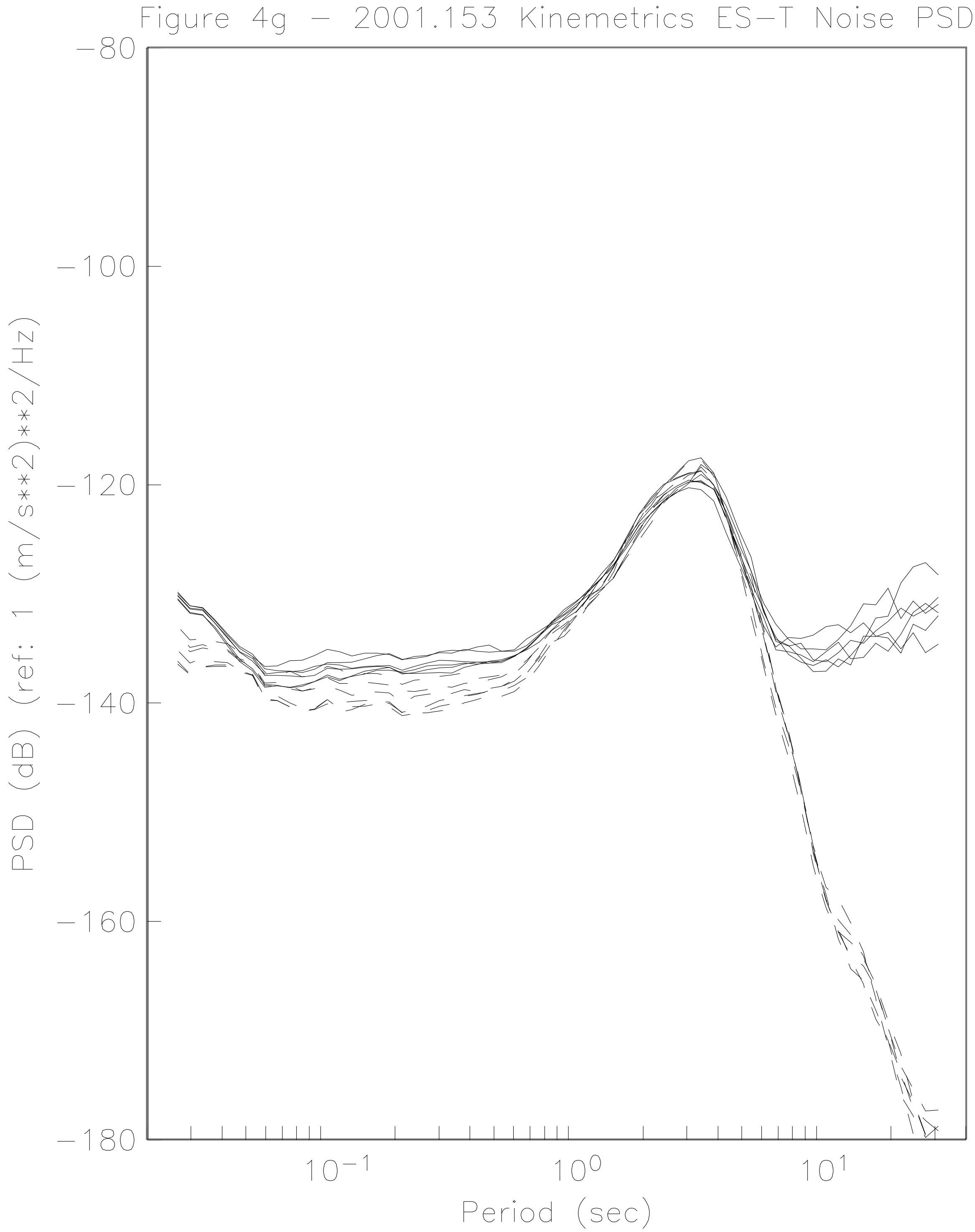
Figure 4g – 2001.153 Kinemetrics ES–T Noise PSD
–80
–100
–120
–140
–160
–180
PSD (dB) (ref: 1 (m/s**2)**2/Hz)
10^{-1}
10^{0}
10^{1}
Period (sec)

Figure 4h - 2001.153 Sensor D Noise PSD

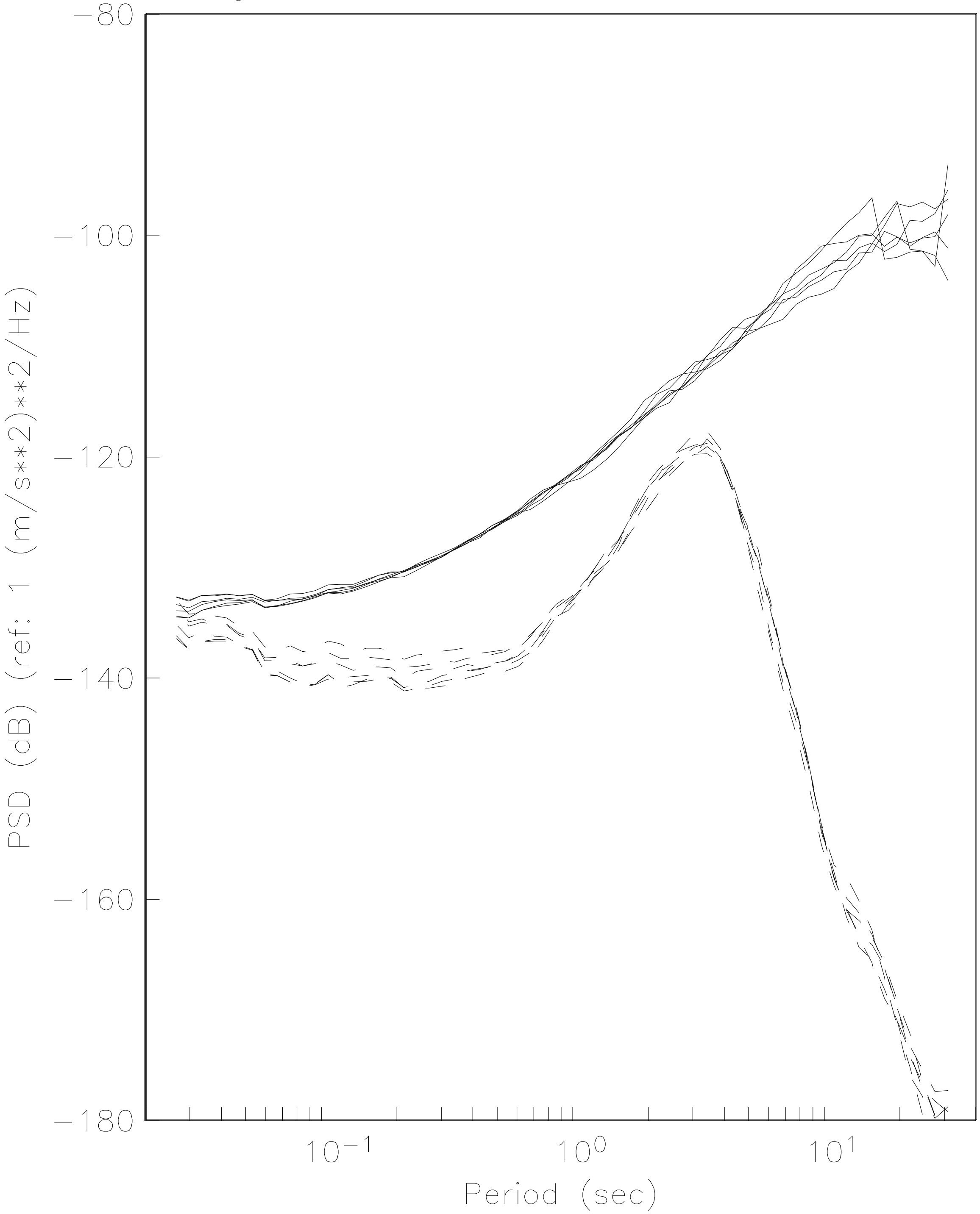

Discussion

The transduction constant for each sensor (see Figure 2) was empirically determined by comparison of the inferred P−wave ground accelerations (see Figure 3) using the STS−2 (±1.5 % calibration accuracy) as the reference. The results were all within 7 percent of the factory supplied constants. The PSD noise plots shown in Figures 4a−h are determined using the empirically derived sensor constants.

Four of the sensors (the Wilcoxon X731B, the PMD MET, the Streckeisen STS−2, and the Kinemetrics Episensor) track the background seismic noise level, observed at BKS, in the ≤0.07 second to ≥7 second period band.

The four sensors with the highest background noise PSD levels (the RefTek 131−02, the Endevco 86, the Applied MEMS SF1500A, and the Wilcoxon 9XL) also happen to be the sensors with the lowest unamplified transduction constants. We are currently running some tests to corroborate this result and to verify that it is not an artifact of the test equipment setup.

We will be testing additional sensors this summer and we will also perform coherency analysis of pairs of the sensors exhibiting the lowest noise PSD levels.